Lagrangian vertical coordinate for UM ENDGame dynamical core

Iva Kavčič, John Thuburn
E-mail: I.Kavcic@exeter.ac.uk

CEMPS, University of Exeter

April 10, 2014

Outline

Outline

What and why

Lagrangian vertical coordinate (LVC)

- Moves with the fluid.
- Keeps track of the height of material surfaces (additional prognostic equation for z (r)).

Why LVC?

- *No need to evaluate vertical departure point.*
- Elimination of vertical advection terms (and associated errors) from the governing equations and numerical model.
- Reduction of horizontal advection errors (if Lagrangian surfaces lie close to isentropes), better Lagrangian conservation properties.

Limitations and further questions

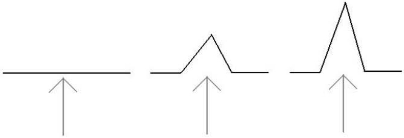

Figure 7: Showing how strong vertical winds can cause folding

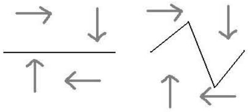

Figure 8: Showing a surface folding into itself

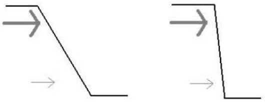

Figure 9: Showing a vertical shear causing folding

- Bending and folding of Lagrangian surfaces over time. [Ken06]
- Difficulty of handling the bottom boundary – use $f(\theta, z)$?
- Reduced vertical resolution in near-neutral stratification.
- Dynamics - physics coupling.

Implementation of LVC in ENDGame

Questions

1. Stability and performance of LVC model for nonhydrostatic compressible Euler equations.
2. Transfer of model fields from old to new levels
   - Re-initialization of Lagrangian surfaces - locations (related to isentropes?), how often?
   - Remapping - which method, what quantities (energy, entropy)?
   - Effect of remapping on conservation (mass, momentum, energy) and stability of the model.
3. Comparison with the current height-based coordinate version of ENDGame.

Equations

$$\frac{D\mathbf{u}}{Dt} - \mathbf{\Psi} = 0 \qquad (1)$$

$$\textit{No vertical advection:} \quad \frac{D\sigma}{Dt} + \sigma\nabla_s \cdot \mathbf{v} = 0 \qquad (2)$$

$$\frac{D\theta}{Dt} = 0 \qquad (3)$$

$$\textit{Additional eqn. for the height of LS:} \quad \frac{Dz}{Dt} = w \qquad (4)$$

$$\mathbf{\Psi} = -2\mathbf{\Omega} \times \mathbf{u} - \theta\nabla\left(\frac{M}{\theta}\right) - \Phi\nabla \ln\theta$$

- Φ - geopotential; $\sigma = \rho\frac{r^2}{a^2}\frac{\partial r}{\partial s}$ - mass (affected by changes in layer depth).
- $M = c_p T + \Phi = c_p \Pi\theta + \Phi$ - Montgomery potential in Helmholtz solver (Π *in height-based ENDGame*).

LVC ENDGame formulation

- LVC coordinate system: $(\xi_1, \xi_2, \xi_3) = (\lambda, \phi, s)$, see [SW03].
- $s \in [0, 1]$, **fixed**: $\dot{s} = 0$ ($s = \eta$ *in HB ENDGame*).
- Variables $F = (r, u, v, w, \theta, \sigma)$.
- Finite-difference: **Lat-lon C-grid** in horizontal, **Lorenz** grid in vertical (*Charney-Philips in the height-based (HB) model*).

Semi-Implicit, Semi-Lagrangian (SISL) scheme, $\alpha + \beta = 1$

$$\mathbf{X}_A^{n+1} - \mathbf{X}_D^n = \Delta t \left[\alpha_{\mathbf{X}} \mathbf{u}_A^{n+1} + \beta_{\mathbf{X}} \mathbf{u}^n \left(\mathbf{X}_D \right) \right], \tag{5}$$

$$F_A^{n+1} - F_D^n = \Delta t \left[\alpha_F N \left(F_A^{n+1} \right) + \beta_F N \left(F_D^n \right) \right]. \tag{6}$$

- $r = a + z$ needs to be recalculated, as well as r depending terms in $\nabla \cdot$, ∇, Coriolis, cell areas and volumes.

Grid and solving

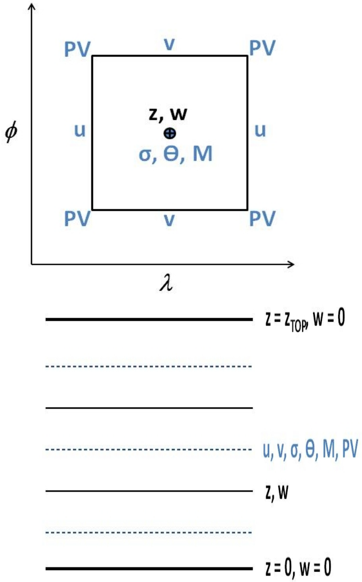

- Centered differences.
- Fixed BC: $z\,(1, i, j) = 0$, $z\,(N + 1, i, j) = z_{TOP}$.
- No flux: $w\,(1, i, j) = 0$, $w\,(N + 1, i, j) = 0$.

Iterative solving:

- $F^{(l+1)} = F^{(l)} + F'$,
- Iterations for $F = (r', u', v', w', \sigma', \theta')$,
- Reference state $F^* = F\,(r)$,
- Helmholtz problem for M' $\Rightarrow$ backsubstitution for F' $\rightarrow$ solutions for F.

Diagnostics: Mass, Energy, Entropy and PV

Total mass (height-based $\rightarrow$ LVC):

$$\mathcal{M} = \int_V \rho dV = a^2 \int_V \rho \frac{r^2}{a^2} \frac{\partial r}{\partial s} \cos\phi d\lambda d\phi ds = a^2 \int_V \sigma A ds \quad (7)$$

Total energy:

$$\mathcal{E} = a^2 \int_V \sigma E A ds, \quad E = c_v T + \Phi + 0.5 \left(u^2 + v^2 + w^2\right) \quad (8)$$

Total entropy:

$$\mathcal{S} = c_p a^2 \int_V \sigma \ln\theta A ds \quad (9)$$

Potential vorticity:

$$PV = \frac{\nabla\theta \cdot \zeta}{\rho} = \frac{\nabla\theta \cdot (\nabla \times \mathbf{u} + 2\mathbf{\Omega})}{\rho} \quad (10)$$

Remapping strategies and methods

Strategies (all not including velocity

- $\mathcal{M}$ and $\mathcal{E}$: remap σ & $\sigma_k E_k \rightarrow$ calculate E_k & θ_k.
- $\mathcal{M}$ and $\mathcal{S}$: remap σ & $\sigma_k \ln \theta_k \rightarrow$ calculate θ_k.
- $\mathcal{M}$ and θ_H: remap σ, $\theta = \theta_H + \theta_{NH}$, interpolate θ_{NH}, $(\sigma)_R \rightarrow \theta_H$ & θ_k.

Methods

- Piecewise parabolic method (PPM, [WA08]).
- Parabolic spline method (PSM, [ZWS06, ZWS07]).
- Edge values estimated from cell averages: **PPM h3, h4, ih4** (**i**mplicit, otherwise explicit).
- Boundary conditions: **d**ecreasing degree of P_n & **o**ne-sided (same degree of P_n, evaluate at different edges).

Outline

Model parameters and initial conditions (IC)

Test cases:

- **Solid body rotation** ($T = 270\,K$; $u = u_0 r \cos\varphi / a$, $u_0 = 40\,m/s$): breaks with energy-conserving Coriolis discretization from the HB ENDGame, runs normally with simple discretization of Coriolis.
- **Baroclinic wave** ([JW06]): $T_0 = 288\,K$, $\Gamma = 0.005\,K/m$, $u_0 = 35\,m/s$, $u'(\lambda, \varphi, s) = u_p \exp\left[-(r/R)^2\right]$.

Parameters:

- Horizontal ($p = 7$): $nx = 2^p = 128$; $ny = 2^{(p-1)} = 64$, $nyp = ny + 1 = 65$ for v.
- Vertical: $z_{TOP} = 32km$, $nz = 32$ (u, v, σ, θ) or 33 (z, w); Uniform ($\Delta z = 1\,km$) or quadratically stretched ($\Delta z = 350\,m$ to $1.2\,km$) grid.
- $\delta_v = 1$, Centered scheme ($\alpha = \beta = 0.5$); Iterations: $n_{out} = 4$, $n_{in} = 1$ (T4x1); $n_{out} = 2$, $n_{in} = 2$ (T2x2).

LVC's bad and good

Table 1: BW case breaking times in days ($p = 7$, $nx = 128$, $ny = 64$, $nz = 32$, uniform grid, $npass = 1$ in Helmholtz solver)

Case \ dt	1200s (20min)	1800s (30min)	2400s (40min)	3600s (60min)
T4x1	30.29	29.44	28.94	28.50
T2x2	29.97	29.27	28.50	26.67
T4x1, u'	7.11	7.27	6.97	6.75
T2x2, u'	6.89	6.88	6.69	6.46

Table 2: Comparison of runtimes in minutes ($dt = 2400s$, $nsteps = 100$, $nz = 32$, uniform grid, $npass = 1$ in Helmholtz solver) for height-based and LVC ENDGame (without and with remapping in every time step).

$n_{out} \times n_{in}$	p	Height-based	LVC	LVC remap
T4x1	7	27:35 (99.8%)	10:29 (99.8%)	11:06 (99.8%)
	6	6:36 (99.8%)	2:34 (99.7%)	2:40 (99.8%)
T2x2	7	15:13 (99.8%)	7:22 (98.6%)	7:52 (99.8%)
	6	3:46 (99.7%)	1:46 (99.7%)	1:54 (99.7%)

BW test case, u' run: LVC z and σ, step 250

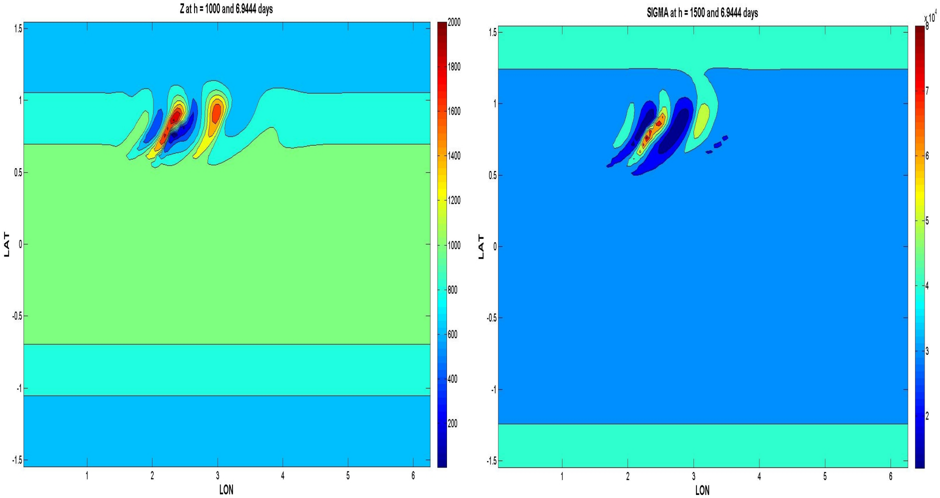

Figure 1: LVC ENDGame, z surface (left), σ surface (right): step 250, uniform grid, T4x1 run, $\Delta t = 2400\,s$, two steps before breaking.

BW test case, u' run: LVC and height–based ρ, step 250

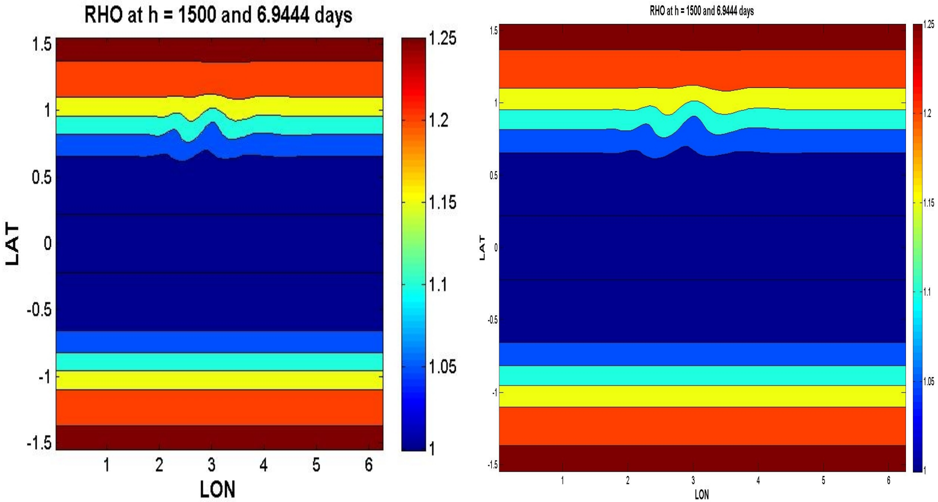

Figure 2: ρ surface (LVC left, HB right): step 250, uniform grid, T4x1 run, $\Delta t = 2400\,s$, two steps before breaking.

BW test case, u' run: LVC and height–based u, step 250

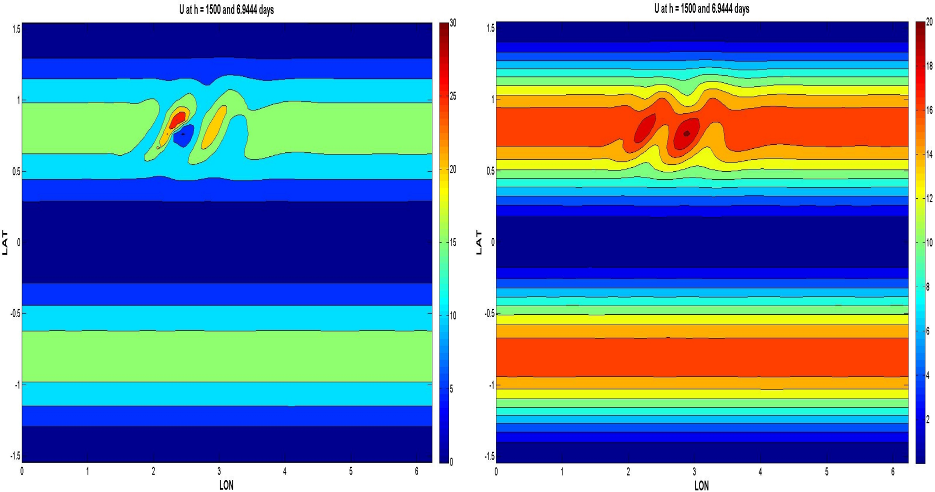

Figure 3: u surface (LVC left, HB right): step 250, uniform grid, T4x1 run, $\Delta t = 2400\,s$, two steps before breaking.

BW test case, u' run: LVC and height–based v, step 250

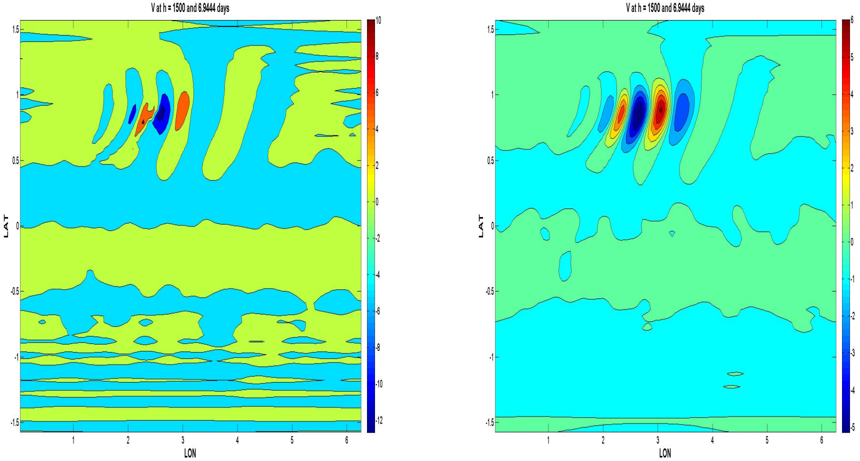

Figure 4: v surface (LVC left, HB right): step 250, uniform grid, T4x1 run, $\Delta t = 2400\,s$, two steps before breaking.

BW test case, u' run: LVC and height–based θ, step 250

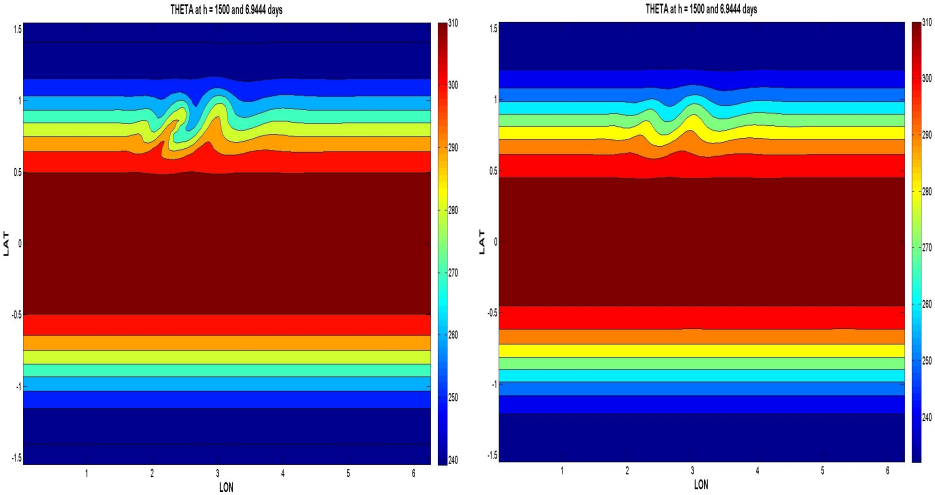

Figure 5: θ surface (LVC left, HB right): step 250, uniform grid, T4x1 run, $\Delta t = 2400\,s$, two steps before breaking.

BW test case, u' run: LVC and height–based PV, step 250

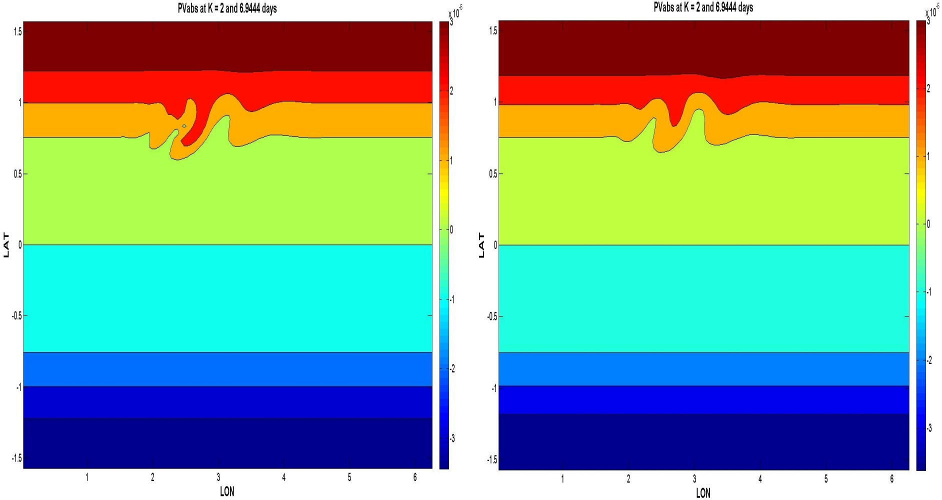

Figure 6: PV surface (LVC left, HB right): step 250, uniform grid, T4x1 run, $\Delta t = 2400\,s$, two steps before breaking.

Application of remapping

- Remapping done column by column, every n timesteps, to initial z levels, (cubic) interpolation for velocity.
- Sum of cell averages (σ, $\sigma_k E_k$, etc.) preserved before and after remapping.
- Different edge values estimators do not really make difference; more often remapping gives better results.

Does not prevent model breaking, just delays it.

Table 3: BW remapping case breaking times in days ($p = 7$, $nx = 128$, $ny = 64$, $nz = 32$, $dt = 1200$, uniform grid, $npass = 1$ in Helmholtz solver), remapping every step.

Case \ Remap	No remap	Energy	Entropy	Hydtheta
T4x1	30.29	39.88	36.81	27.25
T4x1, u'	7.11	10.88	11.06	10.72

BW test case, u' remap run,: LVC σ, step 250

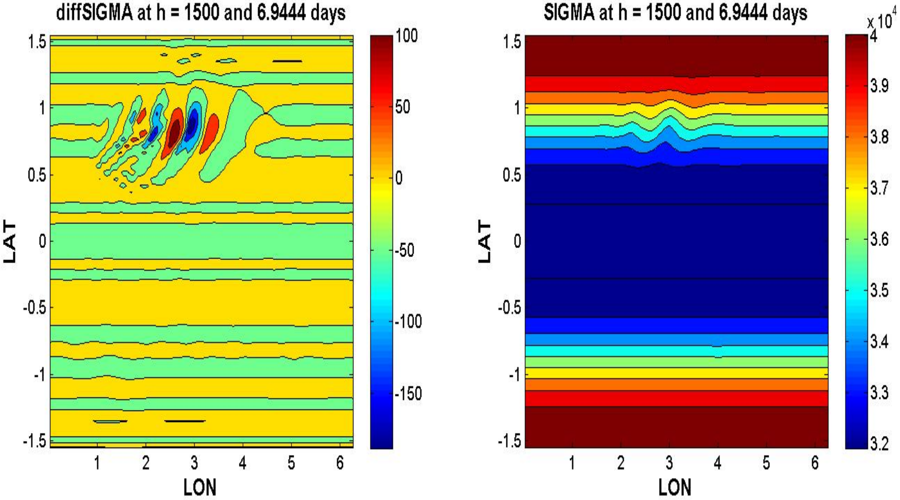

Figure 7: LVC ENDGame, σ surface after (right) energy remapping, and differences (left): step 250, uniform grid, T4x1 run, $\Delta t = 2400\,s$.

BW test case, u' remap run: LVC u, step 250

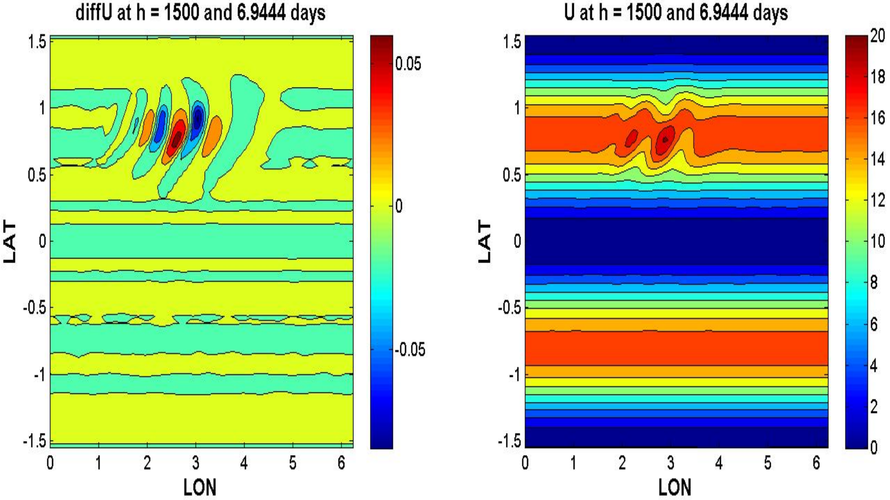

Figure 8: u surface after (right) energy remapping, and differences (left): step 250, uniform grid, T4x1 run, $\Delta t = 2400\,s$.

BW test case, u' remap run: LVC v, step 250

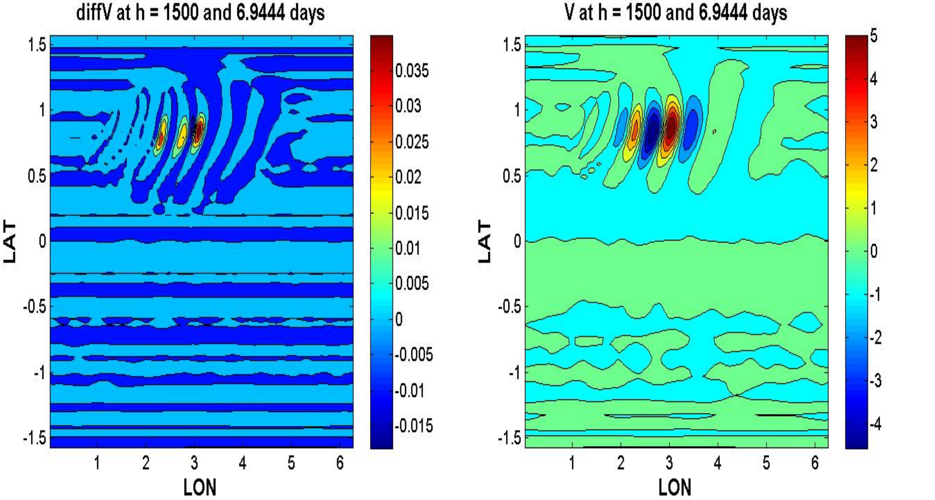

Figure 9: v surface after (right) energy remapping, and differences (left): step 250, uniform grid, T4x1 run, $\Delta t = 2400\,s$.

BW test case, u' remap run: LVC θ, step 250

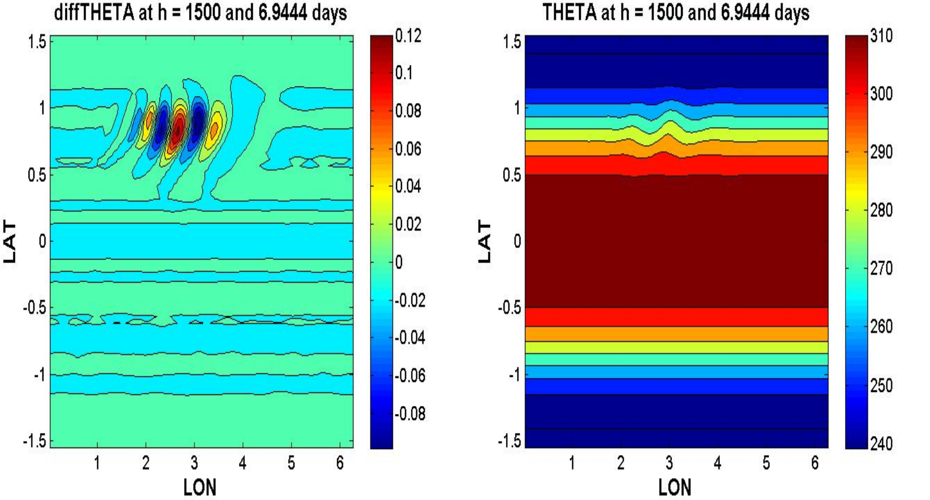

Figure 10: θ surface after (right) energy remapping, and differences (left): step 250, uniform grid, T4x1 run, $\Delta t = 2400\,s$.

Outline

Summary

- Benefits of LVC:
  - No vertical advection calculation, vertical component of departure point predicted $\Rightarrow$ significantly reduced running time in comparison with HB ENDGame.
  - Cost of remapping (so far) not so significant.
- 3D LVC able to maintain SBR with simple Coriolis discretization; breaks for BW case even with the remapping.
- Issues of LVC:
  - Stability for BW case - in formulation, remapping or both?
  - Choice of optimal target levels for remapping (currently to initial levels).

References I

[JW06] C. Jablonowski and D. L. Williamson. A baroclinic instability test case for atmospheric model dynamical cores. *Q. J. Roy. Meteorol. Soc.*, 132:2943–2975, 2006.

[Ken06] J. Kent. Folding and steepening timescales for atmospheric lagrangian surfaces. Master's thesis, University of Exeter, 2006.

[SW03] A. Staniforth and N. Wood. The deep–atmosphere Euler equations in a generalized vertical coordinate. *Mon. Weather Rev.*, 131:1931–1938, 2003.

[WA08] L. White and A. Adcroft. A high–order finite volume remapping scheme for nonuniform grids: The piecewise quartic method (PQM). *J. Comput. Phys.*, 227:7394–7422, 2008.

[ZWS06] M. Zerroukat, N. Wood, and A. Staniforth. The Parabolic Spline Method (PSM) for conservative transport scheme problems. *Int. J. Numer. Meth. Fluids*, 11:1297–1318, 2006.

[ZWS07] M. Zerroukat, N. Wood, and A. Staniforth. Application of the Parabolic Spline Method (PSM) to a multi–dimensional conservative transport scheme (SLICE). *J. Comput. Phys.*, 225:935–948, 2007.